

Enhancing fMRI contrast in awake-behaving primates using intravascular magnetite dextran nanoparticles

David J. Dubowitz,^{CA} Kyle A. Bernheim, Dar-Yeong Chen,¹ William G. Bradley Jr¹ and Richard A. Andersen

Division of Biology, 216-76, California Institute of Technology, Pasadena, CA 91125; ¹Long Beach Memorial MRI Center, Long Beach Memorial Medical Center, Long Beach, CA 90806, USA

^{CA}Corresponding Author

Received 11 April 2001; accepted 25 May 2001

Functional MRI in awake-behaving primates is an emerging tool for bridging the gap between human fMRI and neurophysiology information from nonhuman primates. We report the use of magnetite dextran nanoparticles (Feridex) as a blood-pool agent to enhance fMRI contrast-to-noise (CNR) in primate fMRI. The intravascular half-life of the magnetite dextran was long compared to lanthanide chelates ($T_{1/2} = 198$ min) with shortened T_2 relaxation observed in blood and cerebral cortex. Greater than 3-fold enhancement in the percentage

MR signal change was observed using nanoparticles (13%) compared with conventional BOLD fMRI (4%). The calculated regional cerebral blood volume in macaque primary visual cortex increased 32% with photic stimulation. The increased CNR allows greater flexibility in the design of awake-behaving primate fMRI studies with the potential for improvements in resolution and significantly shortened imaging times. *Neuro-Report* 12:2335–2340 © 2001 Lippincott Williams & Wilkins.

Key words: Cerebral blood volume; Feridex; fMRI; Functional activation; Magnetite; Rhesus macaque monkey; Visual cortex

INTRODUCTION

fMRI is a rapidly emerging tool in the study of primate physiology. Previous studies have addressed the potential value of fMRI in awake macaque monkeys for investigating visual neuroscience [1–5] and basal ganglia function [6]. One major limitation in performing monkey fMRI at 1.5 T is the limited signal-to-noise and consequently low contrast-to-noise ratio (CNR) from blood oxygen level-dependent (BOLD) contrast. As with all imaging techniques, there is a compromise between resolution and sensible imaging time. Monkeys are challenging subjects to study. They need to be trained meticulously to remain still for awake MRI studies (thus shorter imaging sessions facilitate behavioral compliance). However, the brain of a macaque monkey is approximately one-fifth of the size of a human brain [7], so there is also a need for higher resolution than in human fMRI studies. One approach to this has been to do macaque imaging at higher applied magnetic field [3]. While improving the CNR, this also increases the unfavorable susceptibility gradients and artifacts, which scale proportionately with the applied magnetic field. Another approach has been to restrict imaging to anesthetized animals. This allows longer imaging times and reduces movement artifacts, but may also diminish BOLD effect due to the vasodilator effects by anesthetic agents, and consequent changes on cerebral blood flow

(CBF) [8]. The use of anesthesia also excludes cognitive studies for which awake-behaving subjects are required.

We investigated the effect of a blood-pool T_2 contrast agent (i.e. a cerebral blood volume (CBV) technique) on CNR compared with conventional BOLD contrast in awake-behaving primate fMRI experiments. Previous studies have demonstrated the utility of such agents for MRI in rats [9], cats [10] and human subjects [11].

The use of contrast agents has not found much favor in human cognitive studies because this makes the study more invasive, but holds promise for awake animal studies [12]. This is the first time this technique has been applied to awake primate imaging. Techniques that employ a T_2 contrast agent provide images sensitive to changes in regional CBV. This has been shown in rats to change by 20% with neural activation [9,13] and by 25% [11] to 32% [14] in humans. Unlike deoxyhemoglobin susceptibility, the CBV change is not dependent on applied magnetic field [9], and thus this technique provides great scope for improved fMRI contrast even at conventional magnetic fields (1.5 T).

MATERIALS AND METHOD

Animal subjects: Approval for this research was obtained from The Institutional Animal Care and Use Committee, Epidemiology and Biosafety Committees. All imaging was

done on a 1.5 T Siemens Vision MR scanner with 23 mT/m gradients (300 μ s rise time). Awake-behaving studies were done on a 8.5 kg male rhesus macaque monkey (*Macaca mulatta*) lying in a sphinx position within this scanner using a 19 cm circularly polarized knee coil. Contrast excretion measurements were done outside the MR scanner on the same animal. Relaxometry studies were also performed on this monkey and on two additional male macaque monkeys (5.5 kg and 10.5 kg) under isoflurane anesthesia. The technique has been described previously [1,2]. In brief, the animal was transported to the MRI facility in a custom-designed cage. For awake studies he crawled into a short tube so that his legs were accessible for i.v. administration of T_2 contrast agent. The monkey was trained to present his leg to the animal handler and accept an intravascular line into a saphenous vein without sedation or general anesthesia. The monkey then crawled into a larger tube which was transferred to the MRI scanner. The monkey's head was secured to the transmit/receive coil and a screen placed 57.3 cm in front of him (providing a $\pm 22^\circ$ visual field of view). Eye-position tracking was performed using a custom-built shielded video camera placed at the bore of the scanner, which was sensitive in the infrared range, and eye illumination from a circular array of 28 MRI compatible IR light-emitting diodes emitting at 810 nm [15]. Digital signal processing involved a system from ISCAN (Iscan Inc. Cambridge, MA) integrated into a computer running a custom program written with Labview software (National Instruments Corporation, Austin, TX). This set-up allowed eye tracking in complete darkness to an accuracy of within 1° of arc. The animal was trained to remain motionless in the scanner for the duration of the imaging experiment (i.e. while gradient noise was audible) and to fixate on a central fixation point to an accuracy of $< 4^\circ$ visual angle for the duration of the stimulus. He was given a fruit juice reward at the end of each imaging run.

For anesthetized studies, the animal was sedated with 10 mg/kg ketamine and maintained on 2% isoflurane using an anesthetic set-up modified for MRI compatibility.

Contrast agent: For functional imaging studies with T_2 contrast agent we used magnetite dextran nanoparticles (Feridex, Advanced Magnetics Inc, Cambridge, MA) infused i.v. This was given as 4.2 mg Fe/kg (75 μ mol/kg) diluted into 25 ml and infused over 5 min through a 5 μ m filter. Imaging was started within 10 min of completing the infusion (ensuring equilibrium state concentration). For assessment of whole blood clearance, a dose of 2.8 mg Fe/kg (50 μ mol/kg) was used.

MR imaging: BOLD and magnetite-enhanced functional images were acquired using a gradient-echo echo planar imaging (GE-EPI) mosaic sequence. The effective echo time (TE_{eff}) of 50 ms was chosen to approximate the T_2^* of monkey cortex. Isotropic 4 mm resolution was achieved with an FOV of 256 \times 256 mm and a 64 \times 64 matrix. Fourteen 4 mm axial slices of the monkey's entire brain were acquired per repetition of 2000 ms (effective TR = 2000 ms). Forty-five repetitions of the 14 slices were acquired for BOLD experiments and 60 repetitions for magnetite dextran experiments. The first repetition was not used in data

analysis allowing 2 s to ensure steady state. Anatomical images used a 3D Magnetization Prepared Rapid Acquisition Gradient Echo sequence (3D-MPRAGE) with TR/TE = 11.4/4.4 ms, flip angle 12° , inversion time (preparation time) 250 ms and delay time (magnetization recovery time) 600 ms. A 141 \times 141 mm field of view (FOV) was acquired with a 128 \times 128 matrix (zero-padded to 256 \times 256), and 118 phase encode steps made through a 130 mm slab (1.1 mm isotropic resolution). Relaxometry measurements for T_2^* (R_2^*) in cortex used a 2D fast low angle shot (FLASH) sequence (TR 1000 ms, TE 5, 7, 10, 12, 15, 18, 20 ms) as described previously [2]. Relaxometry measurements on *in vitro* venous blood were performed using a CPMG spectroscopy sequence on a Bruker minispec mq60 at 60 Mhz (Bruker Analytik GmbH, Rheinstetten, Germany).

Stimulus paradigm: The stimulus consisted of a 6 s black and white polar checker-board alternating at 8 Hz, which subtended a visual angle of $\pm 20^\circ$. The stimulus was preceded by a 1° fixation point visible for 8 s. Following the fixation dot and checker-board stimulus, the animal remained in the dark for a further 76–106 s to allow acquisition of the full recovery of the hemodynamic response.

Image post-processing: Functional imaging data using BOLD and magnetite dextran contrast were analyzed off-line using AFNI software running on a Unix workstation [16].

Functional images were co-registered using a volume-registration algorithm under AFNI. A weighted linear least squares fit of the images was employed with Fourier interpolation used for resampling [17]. Images with excessive motion artifact not corrected by the registration algorithm were excluded. The remaining runs were averaged together to create a single dataset for BOLD imaging and a single dataset for magnetite-enhanced imaging. A representative region of interest was chosen in primary visual area V1 (Fig. 1). The time course of the percentage change in MRI signal in this volume was plotted for BOLD and magnetite-enhanced fMRI (Fig. 2).

For cerebral relaxometry measurements following magnetite dextran infusion, regions of interest were drawn around anatomically defined gray matter using Scion Image software (<http://www.scioncorp.com>). R_2^* transverse relaxation rate was calculated by assuming an exponential relationship between the MR signal ($S(TE)$), the echo time (TE), and the initial signal ($S(0)$) described by eqn 1:

$$S(TE) = S(0)e^{-TE \cdot R_2^*} \quad (1)$$

The fit optimization was implemented in Matlab (The Mathworks Inc., Natick, MA) using a proprietary large-scale subspace trust-region algorithm based on an interior reflective Newton method [18]. The algorithm allows specification of upper and lower bounds on each optimized parameter.

Relaxivity data on whole blood to assess clearance of contrast media was assumed to follow first order kinetics and was modeled with monoexponential decline described by eqn 2:

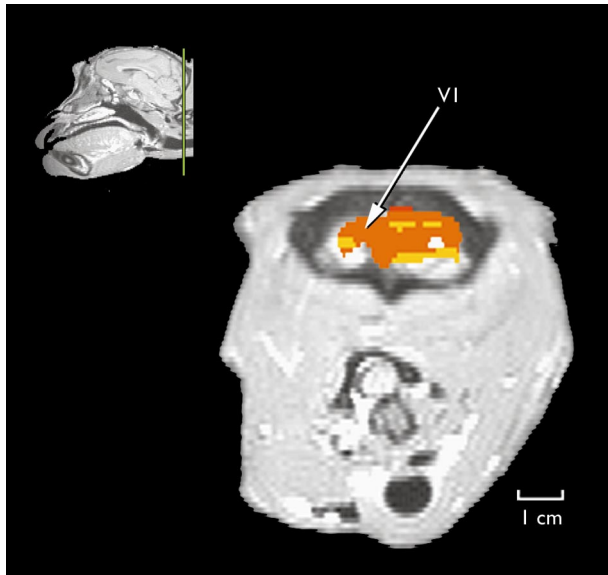


Fig. 1. Coronal image showing functional activation in primary visual cortex (V1) during photic stimulation in a macaque monkey following intravenous T_2 magnetite dextran contrast agent. The plane of section is indicated by the vertical bar on the sagittal image. The area of V1 used to plot MR signal responses is indicated. (Subject's right is on the left of the image.)

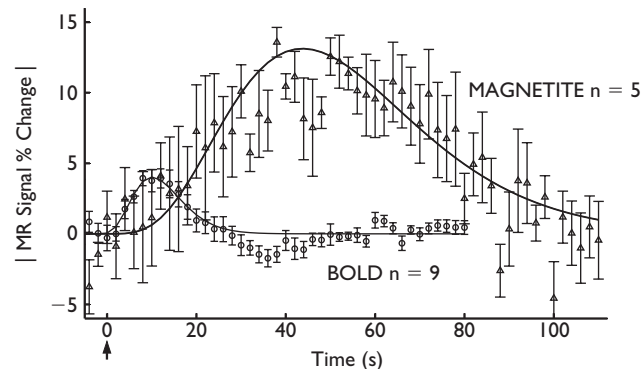


Fig. 2. The time course of the percentage change in MR signal following 6 s photic stimulation is shown for BOLD (circles) and magnetite-enhanced fMRI (triangles). Stimulus onset is indicated by the arrow. Negative MR signal changes for magnetite-enhanced fMRI are shown as positive absolute changes for comparison. Error bars indicate ± 1 s.e. for BOLD ($n=9$) and magnetite dextran ($n=5$) studies. Solid line is the gamma-variate function fitted to the data for the positive BOLD and negative magnetite dextran responses.

$$[Fe]_{blood} = C_0 \cdot e^{-bt} \quad (2)$$

$[Fe]_{blood}$ is the concentration of Fe in blood, C_0 is the instantaneous concentration at time zero. Dividing the injected dose by the instantaneous concentration of contrast media, C_0 , yields the volume of distribution of the agent within the animal. The constant, b , is an excretion constant from which the half-life of elimination from blood can be calculated. There is a linear relationship between the transverse relaxation rate of the magnetite dextran contrast media in blood and the concentration of Fe. The main components of the measured R_2^* are components from

blood itself, $R_2^*_{blood}$, and from exogenous magnetite, $R_2^*_{Fe}$ (eqn 3):

$$R_2^*_{blood} + R_2^*_{Fe} = k \cdot [Fe]_{blood} \quad (3)$$

The unknown contribution to transverse relaxation rate from Fe, $R_2^*_{Fe}$, used in eqn 3, was calculated by making serial dilutions of a known concentration of Feridex with water as described in eqn 4 (Fig. 3a):

$$R_2^*_{water} + R_2^*_{Fe} = k \cdot [Fe]_{water} \quad (4)$$

Using eqns 3 and 4, the actual concentration of Fe was quantified from measurements of R_2^* for whole blood drawn at regular intervals following injection of the contrast agent (Fig. 3b).

To compare the magnitude, duration and onset delay of the positive MR signal change for BOLD with the negative signal change for magnetite-enhanced fMRI, the data were fitted to a gamma-variate function of the form in equation 5 using the same Matlab routine described above:

$$S(t) = A(t - t_0)^r e^{-(t-t_0)/a} \quad (5)$$

A , r , and a are fit constants and t_0 defines the onset delay following the neuronal stimulus. The maximum signal

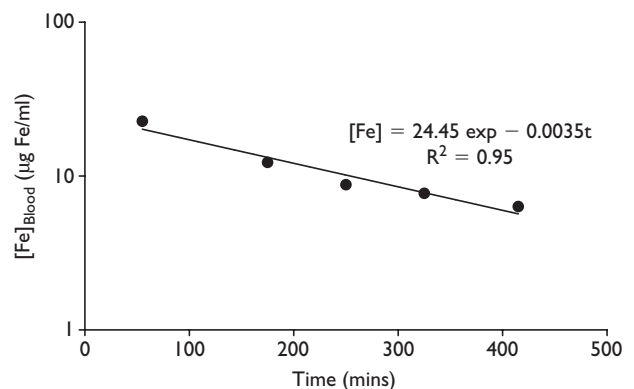
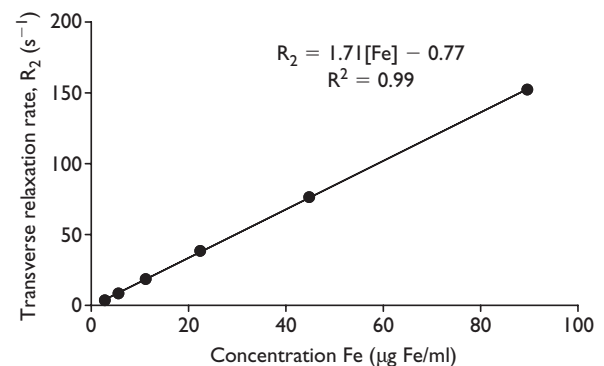


Fig. 3. (a) Linear relationship between magnetite dextran concentration in water and transverse relaxation rate used to calibrate the absolute blood concentration of Fe. (b) Calibrated blood concentration of Fe (semi-log scale) following administration of 2.8 mg Fe/kg (50 $\mu\text{mol/kg}$) magnetite dextran. Excretion follows monoexponential kinetics with a blood half-life of 198 min.

change was the peak of the curve. The duration of activity was compared during the period when the MR signal exceeded 10% of its maximal value.

We calculated the percentage change in the regional CBV following photic stimulation. This model assumes that the effect of the decreased transverse relaxation rate due to BOLD is negligible compared to the increase due to CBV changes with the intravascular contrast agent. Previous studies have shown the rate of change in transverse relaxation rate with blood iron concentration is proportional to the CBV (i.e. the cerebral blood volume $CBV(t)$) can be calculated from the slope of a plot of R_2^* change with $[Fe]_{blood}$ [11]), as described in eqn 6:

$$\frac{R_2^*(t) - R_2^*(0)}{[Fe]_{blood}(t) - [Fe]_{blood}(0)} = K \cdot CBV(t) \quad (6)$$

$R_2^*(t)$ is the transverse relaxation rate during activation or rest, $R_2^*(0)$ is the relaxation rate prior to injection of magnetite dextran, $[Fe]_{blood}(t)$ is the blood concentration of Fe during the photic stimulation experiment, $[Fe]_{blood}(0)$ is the blood concentration of Fe due to magnetite dextran prior to injection (i.e. zero) and K is a proportionality constant.

The fractional change in blood volume following photic stimulation, ΔCBV , can thus be calculated from the CBV during rest, $CBV(r)$, and during activation, $CBV(a)$, from eqn 7:

$$\Delta CBV = \frac{CBV(a) - CBV(r)}{CBV(r)} = \frac{R_2^*(a) - R_2^*(r)}{R_2^*(r) - R_2^*(pre)} \quad (7)$$

From eqn 1, this can be written in terms of the ratio of MR signal during photic stimulation and at rest:

$$\%CBV = \frac{-1}{TE} \cdot \ln\left(\frac{S(a)}{S(r)}\right) \cdot \frac{1}{R_2^*(r) - R_2^*(pre)} \cdot 100\% \quad (8)$$

R_2^* in brain was measured before injection of magnetite dextran, $R_2^*(pre)$, and at regular time points during the experiment, $R_2^*(t)$. This value of $R_2^*(t)$ was interpolated to the actual time point of the photic stimulation measurement, $R_2^*(r)$, to allow for changes in R_2^* due to hepatic elimination of Fe (see eqn 2). The MR signal change, $S(t)$, following photic stimulation was fitted to the gamma-variate function described by eqn 5 (Fig. 2). $S(r)$ was the value of the function at $t < 5$ s and $S(a)$ was the maximum value of the function ($t = 44$ s).

RESULTS

Nine runs of BOLD contrast and five runs of magnetite-enhanced contrast, which were free from any motion artifact, were acquired in an awake-behaving monkey with eye traces confirming he was fixating for the duration of the experiment. The distribution of fMRI activation for the checker-board stimulus is seen in visual cortex in the correlation map in Fig. 1. The hemodynamic response curves for conventional BOLD fMRI and magnetite-enhanced fMRI are shown in Fig. 2. The positive BOLD effect and negative magnetite-induced MR signal changes were fitted to independent gamma-variate functions. Following

photic stimulation, the MR signal in macaque visual cortex is modulated by up to 4% for BOLD imaging and follows a characteristic time course similar to that routinely described in human fMRI at 1.5T. Increase in BOLD MR signal occurred in primary visual cortex almost immediately following stimulus onset. The peak BOLD signal change was observed 10 s following the stimulus onset. The response showed a typical rise followed by an undershoot, returning to baseline by 50 s. The duration of the positive BOLD change (measured between the rise above 10% maximum signal change, to the fall below 10% maximum) was 22 s (1–23 s after stimulus onset). Using i.v. magnetite dextran, there is a 13.1% negative MR signal change in the same area of primary visual cortex following photic stimulation. Maximum effect was seen at 44 s. The modulation in MR signal persisted for 90 s (15–105 s between the 10% of maximum points). The intravenous magnetite dextran, increased the R_2^* (and R_2) relaxation rates in resting gray matter. The change in transverse relaxation rate of blood over time was measured in the same animal used for the fMRI study, and is presented in Fig. 3b. This shows an elimination $T_{1/2}$ from blood of 198 min. The volume of distribution (instantaneous blood concentration divided by dose injected) was 825 ml. The percentage change in regional cerebral blood volume in macaque primary visual cortex following photic stimulation was 32%.

DISCUSSION

Feridex (ferumoxide solution) is an aqueous colloid of magnetite iron oxide nanoparticles (60–150 nm diameter) associated with dextran having an average chemical composition of $FeO_{1.44}$. Excretion of Feridex is 98% hepatic (its primary use in diagnostic imaging is as a T_2 liver contrast agent). In this study we have used it as a blood-pool contrast agent, taking advantage of its slow excretion kinetics and prolonged blood half-life. The blood volume of a 8.5 kg macaque monkey is ~10% of body weight [19], thus the calculated volume of distribution (825 ml) confirms that Feridex is a true blood-pool agent.

fMRI provides an indirect map of neuronal activation by demonstrating changes in cerebral blood dynamics that accompany neural activity. These temporally correlated changes may be seen as changes in blood flow [20], blood volume [14] or changes in the deoxygenation of hemoglobin [21]. Imaging the changes in blood volume is well established: the first fMRI descriptions of neuronal activity in humans mapped changes in CBV [14]. For human studies, it has become more popular to use fMRI studies with endogenous contrast based on changes in the oxygenation of hemoglobin thus making the study entirely non-invasive. The use of iron oxide T_2 contrast agents with a long i.v. half-life has been shown to be a valid method to track CBV changes during neuronal stimulation in rats [9] and human subjects [11]. The increase in transverse relaxation rate ($\Delta R_2^* = 1/\Delta T_2^*$) due to increased blood volume competes with the decrease in relaxation rate due to changes in deoxyhemoglobin accompanying neuronal activation. It is necessary to use a sufficient intravascular concentration of contrast agent to ensure that the signal changes induced by the contrast agent and increased CBV dominate concurrent BOLD changes. At 1.5T these relax-

ivity changes due to hemoglobin susceptibility effects are relatively small; however the observed MR signal changes due to the T_2 agent are less than the theoretical maximum, as these competing effects reduce the magnitude of the MR signal change [9].

The calculated CBV change with stimulation was 32%. This is in good agreement with previous measurements of between 25% [11] and 32% [14] in human subjects. This concordance in CBV changes between human and macaque highlights a similarity in their neurovascular physiology which underscores the value of macaque fMRI as a model for better understanding human neurophysiology.

It is important to consider the decay in R_2^* over time due to hepatic elimination of contrast medium as well as the R_2^* modulation due to changes in blood volume. The elimination half-life of Feridex (198 min) is of the same order of magnitude as the duration of many primate physiology studies. Closer inspection of the intravascular iron concentration during a typical 3.5 h primate imaging session using a dose of 4.2 mg Fe/kg (75 μ mol/kg) shows it ranged from 36.75 μ g Fe/ml (659 μ M) instantaneously following injection to 19.5 μ g Fe/ml (350 μ M). Comparison with previous studies using the same T_2 contrast agent in humans indicates that the BOLD effect due to auditory stimulation is completely negated by the iron-oxide enhanced CBV effect at a concentration of 8.4 μ g Fe/ml (150 μ M) [11]. Extrapolating our elimination curve (Fig. 3) to this point where the BOLD effect completely opposes signal due to exogenous magnetite, indicates that signal would be lost 7 h after injection. During prolonged studies, the contrast concentration will diminish, and the opposing BOLD effect will reduce the MR signal, causing reduced CNR and greater variability. During a typical primate study, the opposing effects on transverse relaxation from BOLD may be assumed to be negligible. Under ideal conditions, the signal change with neuronal stimulation could reflect the whole 32% increase in CBV, thus CNR improvements of 8-fold could theoretically be achieved over our 4% BOLD MR signal change. There is thus scope to improve the MR signal response above the 3-fold enhancement demonstrated here. The use of higher doses is under review. Our TE of 50 ms was initially set for maximum tissue contrast during BOLD studies, and was held constant during the study. Reducing the TE to the T_2^* of grey matter following magnetite dextran infusion would further improve SNR and the CNR observed during magnetite-enhanced fMRI. Additionally, using other iron oxide agents with smaller particle size than Feridex (and a longer elimination half-life and higher T_2 relaxivity characteristics [22]) would further improve the signal benefit over conventional BOLD imaging. The variability of the MR signal change in Fig. 2 is larger for magnetite-enhanced fMRI than for BOLD. This is due to reduction of the resting MR signal by the addition of magnetite dextran. Magnetite reduces the T_2^* of tissue, and thus measured signals for a given TE are lower. The resting MR signal is approximately halved by the addition of magnetite dextran, thus decreasing the SNR.

In non-human primates, the temporal dynamics of the CBV changes are slower than the BOLD effect (similar to that described in rats [9]). This may place some constraints on paradigm design. For block design paradigms, the time-

course of each state may need to be longer than the minimum times typically possible for BOLD studies, however superposition calculations may be used to reduce this increase in experimental time. The use of event-related techniques (currently used in BOLD fMRI to observe temporal changes which are fast relative to the prolonged hemodynamic response [23]) can potentially be applied to CBV imaging as well. The prolonged HRF using magnetite also needs to be considered when directly comparing fMRI with primate electrophysiology. The temporal resolution of MRI is already several orders of magnitude longer than that achievable with single electrode recordings. The advantages of functional MRI is the superior spatial resolution it affords, thus the potential for added CNR (and hence spatial resolution) are likely to outweigh any loss in temporal resolution from CBV techniques. For most primate studies, the 3-fold increase in CNR (with theoretically further increase possible) outweighs many limitations that the slower return to baseline may place on the choice of paradigm. To achieve a comparable 3-fold increase in CNR using BOLD fMRI at 1.5 T would require a 9-fold increase in experiment time or 3-fold increase in voxel size.

The added CNR by using magnetite-enhanced fMRI can be used to improve resolution or shorten total experimentation time. Motion artifact is the major difficulty in imaging awake-behaving primates, and the ability to reduce the number of runs (and the overall length of an experiment) will have dramatic and positive benefits on experimental success. Non-human primate functional neuroanatomy has been used as a model for better understanding the human brain. The smaller brain size may equate to smaller functional units within the cortex for which higher resolution is required (although the exact scaling factor of functional units across species remains to be determined [24]). The ability to achieve higher resolution in primate fMRI also adds to its utility when comparing with neurophysiology data.

The BOLD effect scales between linearly and quadratically with applied field strength [25]. Thus high field imaging at 4.7 T [3] could be expected to afford at least a 3-fold increase in CNR. This theoretical gain needs to be offset by increased bulk-susceptibility artifacts at higher applied magnetic fields. Using magnetite-enhanced fMRI for primate imaging at 1.5 T allows a comparable increase in CNR (with further CNR improvement anticipated with the use of alternate contrast agents), but without the increase in bulk susceptibility distortions induced by higher field. Similar improvements in resolution seen by increasing the applied field strength to 4.7 T are thus achievable using magnetite-enhanced fMRI at 1.5 T.

CONCLUSION

We describe a modification of conventional BOLD fMRI applied to awake-behaving primates. Intravenous infusion of magnetite dextran nanoparticle T_2 contrast agent produces a 3-fold increase in CNR. Opportunities for further optimization are also discussed. Considerably faster overall experiments involving fewer sampling repetitions may now be performed, with the potential for higher resolution imaging compared with existing fMRI techniques at 1.5 T. Regional cerebral blood volume increases by 32% in macaque visual cortex, which is comparable to the neuron-

ally induced vascular changes previously described in humans.

REFERENCES

1. Dubowitz DJ, Chen DY, Atkinson DJ *et al. Neuroreport* **9**, 2213–2218 (1998).
2. Dubowitz DJ, Chen DY, Atkinson DJ *et al. J Neurosci Methods* **107**, 71–80 (2001).
3. Logothetis NK, Guggenberger H, Peled S *et al. Nature Neurosci* **2**, 555–562 (1999).
4. Paradiso MA. *Nature Neurosci* **2**, 491–492 (1999).
5. Stefanacci L, Reber P, Costanza J *et al. Neuron* **20**, 1051–1057 (1998).
6. Zhang Z, Andersen AH, Avison MJ *et al. Brain Res* **852**, 290–296 (2000).
7. Allman JM. *Evolving Brains* New York: Scientific American Library; 1999, p. 256.
8. Seifritz E, Bilecen D, Hanggi D *et al. Psychiatry Res* **99**, 1–13. (2000).
9. Mandeville JB, Marota JJ, Kosofsky BE *et al. Magn Reson Med* **39**, 615–624. (1998).
10. White DL, Aicher KP, Tzika AA *et al. Magn Reson Med* **24**, 14–28. (1992).
11. Scheffler K, Seifritz E, Haselhorst R *et al. Magn Reson Med* **42**, 829–836. (1999).
12. Dubowitz DJ, Bernheim KA, Chen DY *et al. Proc Int Soc Magn Res Med* **1**, 652 (2001).
13. Kennan RP, Scanley BE, Innis RB *et al. Magn Reson Med* **40**, 840–846 (1998).
14. Belliveau JW, Kennedy DN, McKinstry RC *et al. Science* **254**, 716–719 (1991).
15. Dubowitz DJ, Martinez A, and McDowell J. *Proc Int Soc Magn Res Med* **3**, 1691 (1999).
16. Cox RW and Hyde JS. *NMR Biomed* **10**, 171–178 (1997).
17. Cox RW and Jesmanowicz A. *Magn Reson Med* **42**, 1014–1018. (1999).
18. Coleman TF and Li Y. *SIAM J Optim* **6**, 418–445 (1996).
19. Butler TM, Brown BG, Dysko RC *et al. Medical management*. In: Bennett CR and Abee RH eds. *Nonhuman Primates in Biomedical Research: Biology and Management*. London: Academic Press; 1995, pp. 257–334.
20. Kwong KK, Belliveau JW, Chesler DA *et al. Proc Natl Acad Sci USA* **89**, 5675–5679. (1992).
21. Turner R, Jezzard P, Wen H *et al. Magn Reson Med* **29**, 277–279. (1993).
22. Mandeville JB, Moore J, Chesler DA *et al. Magn Reson Med* **37**, 885–890. (1997).
23. Dale AM. *Hum Brain Mapp* **8**, 109–114 (1999).
24. Ahrens ET and Dubowitz DJ. *NMR Biomed*, **14(5)**, 318–324 (2001).
25. Gati JS, Menon RS, Ugurbil K *et al. Magn Reson Med* **38**, 296–302 (1997).

Acknowledgements: We gratefully acknowledge J. Michael Tyszka for enlightened discussion and Betty Gillikin for help with animal handling and health care. This work was funded in part by grants from National Institutes of Health (GM08042 and EY07492) and a James G. Boswell Professorship (R.A.A.).